Forward-backward analysis of fast and slow hadrons in the interactions of ^{6}Li and emulsion nuclei at 3.7*A* GeV

Khaled Abdel-Waged*
Physics Department, Faculty of Science, Benha University, Egypt
(Received 2 November 1998)

A thorough theoretical analysis of fast and slow hadrons emitted in the forward ($\theta<90°$) and backward ($\theta\geqslant 90°$) hemispheres in the interactions of ^{6}Li (3.7*A* GeV) with emulsion nuclei is made with a modified FRITIOF model (which allowance is made for secondary interactions) and a typical cascade model. It is found that, while the cascade model applies well in the region of limited cascading (backward hemispheres), it becomes less applicable in the forward hemisphere (where cascading becomes more branched). The modified FRITIOF model, on the other hand, could reproduce the experimental observations in both hemispheres. [S0556-2813(99)00205-8]

PACS number(s): 25.75.−q, 29.40.Rg

I. INTRODUCTION

Recent results from experiments on relativistic light and heavy ion collisions elucidate the importance of the rescattering and cascading of particles in the spectator part of the nucleus [1–8]. The nucleons participating in the process play an important role in the latter evolution of the collisions. Models that are quite successful in explaining particle production in the region where the projectile and target nuclei overlap normally fail when describing particle yields in fragmentation regions, unless additional assumptions about the later stages of the collisions are made. In order to increase our knowledge of the mechanisms involved, it is evidently of interest to collect precise data on the production of fast and slow projectile-target associated particles.

Recently [7,8], data on the multiplicity distributions of charged particles and their correlations were studied in the backward hemisphere (BHS) ($\theta\geqslant 90°$) as well as in the forward hemisphere (FHS) ($\theta<90°$) for ^{6}Li (3.7*A* GeV) with the use of nuclear emulsion (where θ is the emission angle with respect to the beam axis). The importance of this study is for our understanding of multiparticle production in these two different regions, as the emission of hadrons in the BHS is kinematically restricted (limited cascading) as compared with the emission in the FHS (more branched cascading).

In this work, collisions between light ions are investigated with a simplified cascade picture which contains two main ingredients: (i) the distribution of the nucleons knocked out by hard collisions (the ''wounded'' nucleons), based on a classical Glauber picture [9], and (ii) the description of secondary interactions by soft processes (Reggeon interactions) [10–12], which basically amounts to a cascade in the two-dimensional impact parameter space.

In the first case (hard processes), the colliding nucleons become excited strings as in the FRITIOF model [13]. If the mass of the excited strings is below some critical value (e.g., 1.2 GeV for nucleons), the string is considered a nucleon. Mesons are produced after a certain time when strings and resonances decay. Particles taking part in the primary collisions are allowed to rescatter with other particles by using prescription (ii) above.

This model (referred to as the modified FRITIOF model) was developed in [10,11,1] and was recently applied [1] to an analysis of the general characteristics of particles produced in the interactions of Au and emulsion nuclei at 10.7*A* GeV.

One of the predictions of the modified FRITIOF model is the size (and charge) of the spectator part of the residual nucleus. The latter is normally excited. The deexcitation process of the excited residual nucleus is treated using the simple statistical decay model (SDM) [14].

Thus a two-step model is employed; namely, the modified FRITIOF model for the first fast-stage process is incorporated in the SDM.

In this paper, we systematically apply the modified FRITIOF model and a typical intranuclear cascade model (ICM) [15,16] (which is basically different from the modified FRITIOF model in the way of treating secondary interactions and the excitation energy given to the residual nucleus) to the yields of forward-backward hadrons resulting from the interactions of ^{6}Li (3.7*A* GeV) with emulsion nuclei and discuss which elements in the two models are crucial for describing the production of these hadrons.

The paper is organized as follows: In Sec. II the basic ingredients of the ICM, modified FRITIOF model, and SDM are defined. In Sec. III, a comparison is made between the models calculations and the experimental results of forward-backward charged particles produced in the interactions of ^{6}Li with emulsion nuclei at 3.7*A* GeV. Finally Sec. IV closes with a few conclusions.

II. DESCRIPTION OF THE BASIC MODELS

A. Intranuclear cascade model

In this subsection we outline the basic ideas of the ICM and summarize the most important features.

(i) Initially, the positions of the nucleons of the two colliding nuclei are sampled according to oscillator densities distribution for $A\leqslant 14$ (where A is the mass number of either

*Electronic address: KHELWAGD@FRCU.EUN.EG

the projectile or target) and the Woods-Saxon density for heavier nuclei. In each nucleus, the nucleon momenta are sampled according to zero-temperature Fermi distributions.

(ii) The nuclei are given their initial momenta by Lorentz boosting. Their shapes are accordingly Lorentz contracted.

(iii) The collision proceeds via n elementary interactions between n_p and n_t nucleons from the projectile and target, respectively. The values n, n_p, and n_t are sampled according to Glauber's multiple scattering formalism using the Monte Carlo (MC) algorithm of Ref. [9]. The nucleons which participate in the interaction accept momentum and begin to move in the nucleus. A nucleon i from nucleus A is assumed to move in a straight line through the other nucleus (B), making an interaction whenever it comes close enough to a nucleon j:

$$(b_x+x_i-x_j)^2+(b_y+y_i-y_j)^2 \leqslant (R_{\rm int}+\lambda_D)^2,$$

where $b_{x,y}$ and $x_{i,j}, y_{i,j}$ are the components of the impact parameter vector and the coordinates of the pair, respectively. $R_{\rm int}$ is the strong interaction range (1.3 fm) and λ_D is the de Broglie wavelength of the projectile nucleon.

(iv) The time evolution of the system is determined by considering many independent simulations of the collision process and taking averages over the values of those quantities calculated in each run. All the collisions that take place in the closest time interval are independently processed. A nucleon involved in the interaction is treated as a cascade particle as soon as it undergoes its first interaction.

(v) The momenta of the colliding particles are determined randomly according to the experimental differential cross section. After the first nucleon-nucleon (NN) collision has been completed, straight line motion is resumed and the next possible collision follows in a similar manner and so on. The process continues until all moving particles either escape from the nucleus or are absorbed.

Following the completion of the cascade process, the masses of residual nuclei are determined by product nucleons that have not escaped from the nuclei but which have not been involved in the interaction. Product mesons that have not escaped from the nuclei are taken into account in determining the charges of residual nuclei. The excitation energy of a residual nucleus is given by the sum of the energies of particles absorbed by the corresponding nucleus and the energies of holes formed in this process.

In addition to this picture, several features are added. First, pion production is introduced by considering the inelastic NN cross section. Second, the Pauli principle and energy-momentum conservation are obeyed in each intranucleon interaction. Third, the so-called trailing effect (rearranging the density) is included; when, for example, a target nucleon is scattered as a result of being in a collison with the projectile, the whole target density is depleted by one nucleon.

The parameters of the ICM model were determined as a result of an analysis of hadron-nucleus (hA) interactions [17,18]. We do not change these values in our calculations. The remaining details of the model can be found in [16]. The sample of generated events consists of 5.0 thousands of interactions for each projectile-target combination. In comparison with the experimental data we applied the same definitions and conditions.

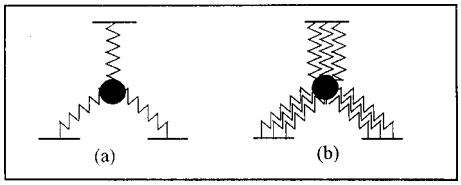

FIG. 1. (a) An enhanced diagram, which represents the interaction of a projectile hadron (solid curve) with two target nucleons (solid curves) through Reggeon splitting (wavy lines) into two. Solid circles represent Reggeon interaction vertices. (b) An enhanced diagram of the ''fan'' type.

It should be noted here that the above model applies to the situation where binary scattering is important and is recognized as the best model applied for smaller projectiles interactions with heavy nuclei in the intermediate energy range [(1–10)A GeV) [19,20].

B. Modified FRITIOF model

In Refs. [10–12], we have shown that the description of the cascading of particles can be achieved in the framework of Regge theory. Each interaction of the incident hadron with nucleons of a target nucleus is assumed to initiate a cascade of Reggeon exchanges. This picture is taken into account in Regge theory. In this theory the interaction of secondary particles with a nucleus is described by cuttings of enhanced diagrams, i.e., diagrams with an interaction between Reggeons. It was shown that inelastic rescatterings occur for any secondary particles, both slow and fast ones, and the yield of enhanced diagrams leads to the enrichment of the spectrum by slow particles in the target fragmentation region.

As in Ref. [21] we shall assume that the Reggeon interaction vertices are small. Therefore of the full set of enhanced diagrams the only important ones will be those containing vertices where one of the Reggeons splits into several, which then interact with different nucleons of the nucleus [Fig. 1(a)]. In studying interactions with nuclei, however, it is convenient, in the spirit of the Glauber approach, to deal not with individual Reggeons, but with sets of them interacting with a given nucleons of the nucleus [Fig. 1(b)]. Unfortunately, the Regge method of calculating the sum of the yields of enhanced diagrams in the case of hA and nucleus-nucleus (AA) interactions is not developed for practical tasks. Hence a simple model of estimating Reggeon cascading in hA and AA interactions is proposed [10].

The yield of the enhanced diagram of Fig. 1(b) is given by

$$Y_c = G\int_{\epsilon}^{Y-\epsilon} d\xi' d^2b' F_{N\pi}(\vec{b}-\vec{b}', Y-\xi') \times F_{\pi N}(\vec{b}'-\vec{s}_1, \xi') F_{\pi N}(\vec{b}'-\vec{s}_2, \xi'), \quad (1)$$

where G is the three Reggeon vertex constant, $Y=\ln s$ is the rapidity of the projectile hadron, ϵ is the cutoff parameter, $F_{\pi N}$ is the amplitude of πN elastic scattering, $\vec{b}$ is the impact parameter of incident hadron, $\vec{s}_1$ and $\vec{s}_2$ are impact coordi-

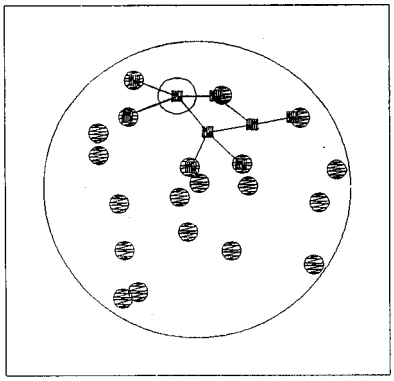

FIG. 2. Reggeon ''cascade'' in hA scattering in the impact parameter plane. The position of the primary interacting nucleon is marked by an open circle, the positions of nuclear nucleons by closed circles, the set of individual Reggeon exchanges by small straight lines, and the square points are the coordinates of the Reggeon interaction vertices.

nates of two nuclear nucleons, and $\vec{b'}$, ξ' are coordinates of Reggeon splitting vertices in the impact parameter-rapidity space. Using Gaussian parametrization for $F_{\pi N}$ [$F_{\pi N}=\exp(-|\vec{b}|^2/R_{\pi N}^2)$] and neglecting its dependence on energy, we obtain

$$Y_c \simeq G(Y-2\epsilon)\frac{R_{\pi N}^2}{3}\exp\{-[\vec{b}-(\vec{s}_1+\vec{s}_2)/2]^2/3R_{\pi N}^2\} \times \exp[-(\vec{s}_1-\vec{s}_2)^2/2R_{\pi N}^2], \quad (2)$$

where $R_{\pi N}$ is the radius of the π N interaction. [Formula (2) assumes that the nuclear size is much greater than the range of hadron-nucleon interactions.] As seen from Eq. (2), Y_c is independent of the longitudinal coordinates and the multiplicity of the produced particles; that is, cascading occurs in the impact parameter plane, and not in the three-dimensional space of the nucleus. This is the main difference between Reggeon cascading and the usual cascading. Schematically, the process can be represented as in Fig. 2.

At large $\vec{b}$, the first exponent of Eq. (2) can be considered (in a crude approximation) as an effective amplitude of the interaction of the projectile hadron with the first nuclear nucleon. In this case the second exponent on the right-hand side of expression (2) has to be treated as the probability of involving the second nucleon in the interaction. Having in mind the weak dependence of the AA-interaction characteristics on the form of the NN elastic scattering amplitude, we neglect the difference between the NN amplitude and the effective one.

In line with these considerations, an algorithm which makes allowance for generating the Reggeon exchange diagrams was formulated [10] as follows.

(1) Nucleon coordinates of the two colliding nuclei were simulated according to a Gaussian distribution for $A \leqslant 14$ and a Woods-Saxon distribution for $A>14$, where A is the mass number of either the projectile or target nucleus.

(2) The impact parameter is simulated according to [9].

(3) At a given impact parameter, the primary interacting or ''wounded'' nucleons of the nuclei were identified by Glauber approximation [9].

(4) Target and projectile spectator nucleons (i.e., those nucleons which have not been involved in the interaction) are then followed. If the i^{th} spectator of nucleus A is at $b_{ij}=\sqrt{(x_i-x_j)^2+(y_i-y_j)^2}$ distance from the j^{th} wounded nucleons of A, the i^{th} nucleon is regarded as a participant of the collisions with probability $w=ce^{-b_{ij}^2}$, $c=0.25$.

(5) If the number of newly involved nucleons is not zero, then step (4) is repeated; otherwise, step (6) is carried out.

(6) The number of spectator nucleons (A_{res}) and the sum of all charges (Z_{res}) are determined. These quantities were identified as the mass number and charge of the nuclear residue.

Basically, this model differs from models that incorporate cascading (e.g., [3, 16, and 22]) by secondary collisions, which in the latter correspond to the rescattering of the ''wounded'' nucleons (i.e., the nucleons which suffer elastic or inelastic scatterings in the first impact) in ordinary (three-dimensional) space on a basis of a collision cross section and mean free path picture. From the Regge approach the cascade of Regge exchanges occurs in two-dimensional space (on the plane of impact parameter) of the target nucleus (see Fig. 2). Thus we expect that the Regge cascade will be more restricted than it is in the usual cascade models.

In the original FRITIOF model, the primary NN collisions are determined using the Glauber approximation. When two hadrons collide, momenta are exchanged and two longitudinally excited objects are created. The excited objects hadronize independently according to the Lund model of jet fragmentation. The hadronization is assumed to take place outside the nuclei and thus no intranuclear cascading is considered.

In order to include cascading in the FRITIOF model, the primary interacting nucleons are allowed to rescatter through Regge cascading (as outlined above). The combination of FRITIOF primary NN scatterings and Regge cascading will be referred to as the modified FRITIOF model.

Each primary inelastic NN collision proceeds in the FRITIOF model as follows: $a+b \rightarrow a'+b'$, where a' and b' are the excited states of the two hadrons (a and b). In the center-of-mass system light cone variables are used,

$$P_+=E+p_z \quad \text{and} \quad P_-=E-p_z,$$

for a hadron moving along the $+z$ and $-z$ axes, respectively (the z axis is taken as the collision axis). E and p_z are the energy and the longitudinal momentum component for each hadron. The probability distribution for the total transfer can be written as

$$dW=\frac{dp_-^{a'}}{p_-^{a'}}\frac{dp_+^{b'}}{p_+^{b'}}. \quad (3)$$

In order to take the excitation (increasing mass of the string object) and deexcitation (decreasing mass of the string) processes into account, the variables $P_-^{a'}$ and $P_+^{b'}$ are allowed to vary in the intervals

$$[E_a - p_{az}, \sqrt{s_{ab}} - m_b] \quad \text{and} \quad [E_b - p_{bz}, \sqrt{s_{ab}} - m_a]. \tag{4}$$

Expressions (4) are calculated at $\sqrt{s_{a'b'}} = \sqrt{s_{ab}} = E_{a'} + E_{b'} = E_a + E_b$, $m_{a'} = m_a$, and $m_{b'} = m_b$. After the collision, the masses of the two excited hadrons are calculated by

$$P_+ P_- = m_\perp^2 = m^2 + p_x^2 + p_y^2. \tag{5}$$

The two longitudinally excited objects are given an average square of transverse momentum equal to 0.3 $(\mathrm{GeV}/c)^2$.

The Fermi motion of the nucleons in the nucleus is taken into account using the algorithm in [23] and energy-momentum conservation is enforced in primary collisions.

In the case of two nuclei A and B, the i^{th} constituent nucleon of nucleus A is fully characterized by the variables

$$x_i^+ = \frac{E_i + p_{zi}}{W_A^+} \quad \text{and} \quad p_{i\perp} \tag{6}$$

and the j^{th} constituent nucleon of nucleus B by

$$y_j^- = \frac{E_j + q_{zj}}{W_B^-} \quad \text{and} \quad q_{j\perp}, \tag{7}$$

where $W_A^+ = \Sigma_{i=1}^A (E_i + p_{zi})$ and $W_B^- = \Sigma_{j=1}^B (E_j + q_{zj})$. Here E_i (E_j) and p_i (q_j) are the energy and the three-momentum of the i^{th} (j^{th}) constituent from A (B). By using these variables and applying the energy-momentum conservation laws

$$\sum_{i=1}^A E_i + \sum_{j=1}^B E_j = E_A^0 + E_B^0,$$

$$\sum_{i=1}^A p_{zi} + \sum_{j=1}^B q_{zj} = p_{zA} + q_{zB},$$

and

$$\sum_{i=1}^A p_{i\perp} + \sum_{j=1}^B q_{j\perp} = 0,$$

we obtain

$$p_{zi} = \left(W_A^+ x_i^+ - \frac{m_{i\perp}^2}{x_i^+ W_A^+} \right) \Big/ 2, \tag{8}$$

$$q_{zi} = -\left(W_B^- y_j^- - \frac{\mu_{j\perp}^2}{y_j^- W_B^-} \right) \Big/ 2, \tag{9}$$

where $m_{i\perp}^2 = m_i^2 + p_{\perp i}^2$, $\mu_{j\perp}^2 = \mu_j^2 + q_{\perp j}^2$, and m_i (μ_j) is the mass of the i^{th} (j^{th}) constituent nucleon from nucleus A (B). It can be seen from Eq. (8) that a choice of (x_i^+) close to zero corresponds to a particle moving in the backward direction, i.e., $-z$ direction. The value of x_i^+ (y_j^-) is chosen according to the distribution

$$dP \sim \prod_{i=1}^A e^{-(x_i^+ - 1/A)^2/d^2} \delta\left(1 - \sum_{i=1}^A x_i^+\right) dx_i^+, \tag{10}$$

where $d = 0.05$. This distribution is defined by fitting the average emission angle of evaporated singly and multiply charged nuclear fragments (black particles) [24–26]. The value of $p_{i\perp}$ $(q_{j\perp})$ is simulated according to

$$dP \sim \prod_{i=1}^A e^{-(p_{i\perp}^2/\langle p_\perp^2 \rangle)} \delta\left(\sum_{i=1}^A p_{i\perp}\right) dp_{i\perp}, \tag{11}$$

where $\langle p_\perp^2 \rangle = 0.05$ $(\mathrm{GeV}/c)^2$.

The sum of transverse momenta gives Fermi motion to the nucleons of the nucleus A (B).

As for the wounded nucleons (which are determined either from the Glauber approach or Regge cascading) the values of $[x_i^+, p_{i\perp}]$ and $[y_j^-, q_{j\perp}]$ are simulated using the distributions (10) and (11) at $\langle p_\perp^2 \rangle = 0.3$ $(\mathrm{GeV}/c)^2$ and $d = 0.21$.

To calculate the excitation energy of the nuclear residuals, it is assumed [11] that each spectator nucleon placed at a distance less than 2 fm from a wounded nucleon (experiencing either a primary or secondary collision) receives an energy distributed as

$$F(E_{\text{ex}}) = \frac{1}{\bar{E}} \exp\left(\frac{-E_{ex}}{\bar{E}} \right), \tag{12}$$

where $\bar{E}$ is the average energy per NN collision. The most recent results [27] obtained from an analysis of Au on Au and Cu at 600A MeV show that the experimentally determined excitation energies are close to the mean binding energy of nuclei (between 8 and 10 MeV). As in [12] we fix the value of $\bar{E}$ at 8 MeV. The sum of the energies transferred to the spectator nucleons gives the excitation energy to the residual nucleus.

It should be noted that the same values of parameters have been used in [1] when discussing the production of particles from the interaction of Au and emulsion nuclei at 10.7A GeV.

C. Statistical decay model

At the end of the first fast stage of the reaction, the ICM and modified FRITIOF simulations yield residual nuclei which are normally excited. The excited residues are allowed to emit nucleons and light fragments if the excitation energy of the residual nucleus is higher than the separation energy.

Though many sophisticated decay codes have been proposed so far, we use here the simple model of light particle evaporation. We consider only n, p, d, t, ^{3}He, and ^{4}He evaporation.

The evaporation probability for a particle of type (j), mass m_j, spin s_j, and kinetic energy E is given by

$$P_j(E)dE = \frac{(2s_j + 1)m_j}{\pi^2 \hbar^3} \sigma_{\text{inv}} \frac{\rho_f(U_f)}{\rho_i(U_i)} E dE, \tag{13}$$

where ρ's are the nuclear level densities $[\rho_f(U_f)]$ for the final nucleus, $\rho_i(U_i)$ for the initial one, U_i is the excitation energy of the evaporating nucleus, U_f of the final one, and σ_{inv} is the inverse cross section for the inverse process.

We use the following simple form for $\rho(U)$ [28]:

$$\rho(U) \simeq C e^{2\sqrt{aU}},$$

with $a = A/8$ MeV^{-1}. The inverse reaction cross section has been parametrized in a simple way so that expression (13) can be analytically integrated and used for MC sampling.

The excitation energy (U) in Eq. (13) is given by

$$U = E_{\rm ex} - E - Q, \tag{14}$$

where $E_{\rm ex}$ denotes the excitation energy of the residual nucleus calculated from Eq. (12). Q is the Q value of the reaction.

The energy spectrum of the emitted particles is obtained by integrating the available energy of Eq. (13) as

$$N(E_j)dE_j = \frac{E_j - U_j^c}{T_j^2} e^{-(E_j - U_j^c)/T_j} dE_j, \tag{15}$$

with $aT_j^2 = E_{ex} - U_j^c - Q_j$ and U_j^c is the Coulomb barrier of the particle j. The statistical decay process is simulated by making use of the Monte Carlo model until no more particles can be emitted.

III. RESULTS AND DISCUSSION

A. Multiplicity distributions

There are only a few experiments known to us in which targets associated particles with nuclear projectiles are investigated. The most detailed results are obtained in experiments using emulsion targets.

The major constituents of the nuclear emulsion are hydrogen (39.5%), carbon (17.7%), nitrogen (4.96%), oxygen (11.9%), bromine (12.9%), and silver (12.9%). The percentage given after each element is the reaction percentage in ^{6}Li (3.7A GeV) induced reactions [7,8].

Hadrons produced in AA interactions at high energy may originate from two mechanisms. They may participate only in the primary reaction and leave the overlap region of projectile and target without further interactions. In emulsion experiments such hadrons are seen as shower tracks (s particles), having $v/c \geq 0.7$. Or they may be involved in the rescattering process by knocking out further nucleons while penetrating through the spectator parts of the nuclei. The intranuclear cascade is responsible for knocking out cascade protons and neutrons of the nuclear remnants. Most of the cascade protons have energies typical for the so-called gray prongs (g particles), having $0.3 \geq v/c < 0.7$.

Both primary and secondary interactions contribute to the excitation of the residual nuclei. In peripheral AA interactions the deexcitation of the residual nuclei proceeds via evaporation of nucleons and light fragments (d, ^{3}H, ^{3}He, α) until a stable configuration is reached. In emulsion such particles are seen as black tracks (b particles), having $v/c < 0.3$.

Table I gives the experimental average values of s, g, and b particles in the forward and backward hemispheres for the interactions of ^{6}Li with emulsion nuclei at 3.7A GeV together with the predictions of the modified FRITIOF model and ICM.

Our results are superposition of multiplicities obtained with hydrogen and light and heavy nuclear targets weighted with fractions corresponding to the emulsion composition used in the experiment. Furthermore, we apply the definitions for ''shower,'' ''gray,'' and ''black'' as given by the experiment. Shower particles are predominately charged pions with an admixture of kaons and protons, having kinetic energy >400 MeV. Gray particles are protons, pions, and kaons with kinetic energy between 26 and 400 MeV. Black particles are singly and multiply charged nuclear fragments having lower energies than the gray particles.

TABLE I. The values of the average multiplicities of the emitted particles in the forward (up) and backward (down) hemispheres for the interactions of ^{6}Li with emulsion nuclei at 3.7A GeV. Results of the modified FRITIOF model and ICM (given in parentheses) are compared with data [7,8].

Forward	$\langle N_s^f \rangle$	$\langle N_g^f \rangle$	$\langle N_b^f \rangle$
Experiment	5.71 ± 0.15	2.08 ± 0.08	2.84 ± 0.09
Modified FRITIOF	(5.61)	(2.67)	(2.27)
ICM	(4.56)	(3.16)	(1.79)
Backward	$\langle N_s^b \rangle$	$\langle N_g^b \rangle$	$\langle N_b^b \rangle$
Experiment	0.41 ± 0.02	0.98 ± 0.05	2.19 ± 0.07
Modified FRITIOF	(0.48)	(0.62)	(1.83)
ICM	(0.30)	(1.05)	(1.43)

From the analysis of the above results one notices that the average values of s and g particles in the FHS are higher than the corresponding values in the BHS. In the case of b particles these values are nearly the same in both hemispheres, reflecting the isotropic nature of the system emitting b particles.

As seen from the table, the average values of s particles emitted in the FHS ($\langle N_s^f \rangle$) and BHS ($\langle N_s^b \rangle$) are reproduced well by the modified FRITIOF model. The $\langle N_s^{f(b)} \rangle$ according to the ICM calculations is about 22% below the experimental observation.

The ICM average value of g particles in the BHS ($\langle N_g^b \rangle$) is in good agreement with the measured value. As for the average value of the forward g particles ($\langle N_g^f \rangle$), the calculated ICM value is in excess of the measured one. Although the ICM underestimates the number of forward-produced particles (low value of $\langle N_s^f \rangle$), there is a more branched cascade (high value of $\langle N_g^f \rangle$).

In the modified FRITIOF model, increasing the number of recoil protons gives rise to a softening proton spectrum in the laboratory system of NN collisions. As one can see, the modified FRITIOF calculations agree with the measured $\langle N_g^f \rangle$, but predict less $\langle N_g^b \rangle$ than that experimentally measured.

The modified FRITIOF average values of forward-backward b particles ($\langle N_b^f \rangle$ and $\langle N_b^b \rangle$) are the nearest to the experimental results while the ICM underestimates the average value of $\langle N_b^{f(b)} \rangle$ (in spite of the fact that the mechanism of decay of the residual nucleus is the same, both using the same SDM).

Figure 3 represents the normalized experimental multiplicity distributions of s, g, and b particles in the forward and backward hemispheres for ^{6}Li (3.7A GeV) interactions with emulsion nuclei along with the results obtained by

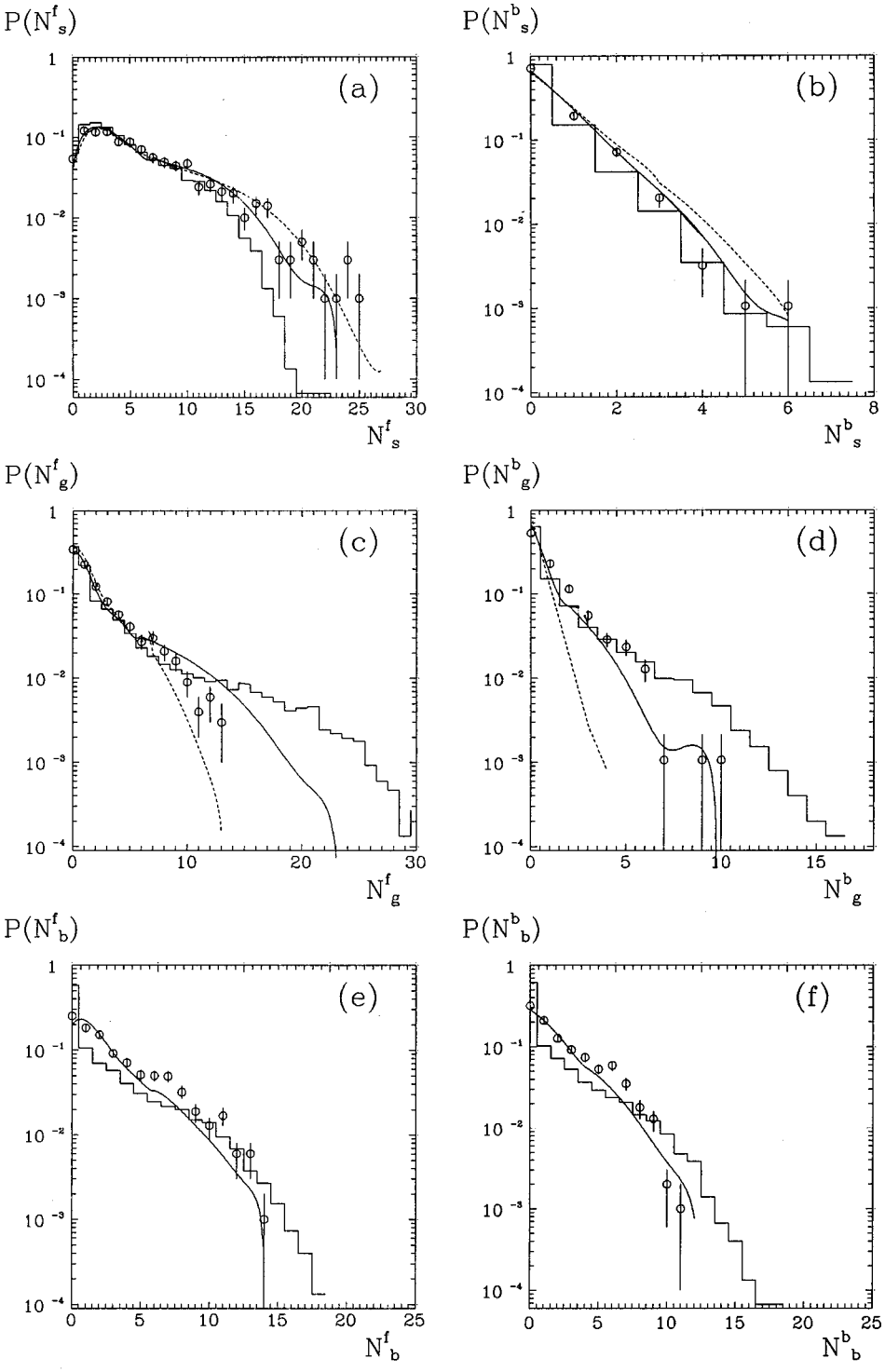

FIG. 3. The normalized experimental multiplicity distributions (error bars) of s, g, and b particles (from top to bottom) produced in the forward [(a), (c), and (e)] and backward [(b), (d), and (f)] hemispheres for ^{6}Li and emulsion nuclei (3.7A GeV) as compared with ICM (histograms) and modified FRITIOF (solid and dashed curves) calculations.

the ICM and modified FRITIOF model. In both calculations we have normalized the distributions to unity and applied the previously given definitions for forward and backward s, g, and b particles.

Figure 3(a) shows that the multiplicity distribution of s particles in the BHS $[P(N_s^b)]$ is reproduced by both models.

The multiplicity distribution of s particles in the FHS $[P(N_s^f)]$, Fig. 3(b), is described well by the ICM calculations except for the high multiplicity tail, where the yield predicted by the ICM is smaller than that observed. The modified FRITIOF model gives a good description of the whole N_s^f distribution.

It should be noted that in both calculations the probabilities of interactions with different components of emulsion are determined according to the Glauber approach. Hence the difference in models predictions is governed by different mechanisms of the multiparticle production process.

The dashed curves in Figs. 3(a) and 3(b) represent the modified FRITIOF calculations by setting $p_{az}=p_{bz}=0$ in Eq. (4), corresponding to maximum string excitations. In the modified FRITIOF model, maximum excitations of the strings are achieved by increasing the number of collisions until the two colliding string objects come to rest in their center-of-mass frame. As seen from Fig. 3(a), the effect of the pro-

cesses appears for large N_s^f values, indicating interactions with heavy target components. The deexcitation processes result in an excess number of pions in the whole N_s^b distribution [see Fig. 3(b)].

Figure 3(c) illustrates that the multiplicity distribution of g particles in the forward hemisphere $[P(N_g^f)]$ calculated by the ICM is in qualitative agreement with the experimental one for $N_g^f<10$. According to the ICM, g particles are mainly produced at the fast stage of the interaction. As seen from the figure, the ICM affords an essential breakup of the heavy target nuclei ($N_g^f>10$) at the fast stage of the interaction, which is due to the great number of intranuclear collisions. The modified FRITIOF model gives a better description of the N_g^f distribution.

In the BHS, Fig. 3(d), the modified FRITIOF calculations of the probability of backward g particles $[P(N_g^b)]$ rapidly decrease with increasing N_g^b as compared with ICM results.

The dashed curves in Figs. 3(c) and 3(d) represent modified FRITIOF calculations by neglecting the Fermi motion of the nucleons in the nucleus. As seen from Fig. 3(c), the absence of Fermi motion prevents a correct description of the emission of g particles in the BHS. As for the FHS [see Fig. 3(d)], the effect reflects only the large N_g^f values ($N_g^f>7$).

The ICM calculations of the multiplicity distributions of b particles in the forward $[P(N_b^f)]$ and backward $[P(N_b^b)]$ hemispheres, Figs. 3(e) and 3(f), provide an inadequate picture of the distributions for $N_b^{f(b)}<7$. The modified FRITIOF model describes rather well the whole b-particle distributions in the two hemispheres.

Bearing in mind the fact that both calculations use the same SDM, one can conclude that the discrepancy is caused by the wrong link of the fast and slow stages of the interactions. As known, the ICM assumes the average nuclear field to be invariable and the excitation energy of the nuclear residues is determined by the Fermi degenerate gas approximation. Such a picture is seemingly incorrect for interactions accompanied by a strong breakup of the nucleus. Thus our model of breakup and excitation of nuclei is more realistic than that given by the ICM.

B. Multiplicity correlations

In AA interactions, a more sensitive characteristic to understand the mechanism of backward production is the correlation between the multiplicities of the different types of the emitted particles. The BHS is intimately connected to the target fragmentation region, i.e., to that part of the phase space where all single-particle characteristics are most safe from being dependent on the projectile mass number. Therefore, it is convenient to study the correlation between the average multiplicities of the different emitted particles and those quantities related to the BHS (target fragmentation region). It is customary to take the multiplicities of N_g^b and N_b^b as indirect measures of these quantities.

The correlations between g and s particles are very important due to their mutual dependence on the number of struck nucleons.

It can be seen from Fig. 4 that the average number of s particles in the FHS sharply increases with increasing the number of backward g particles up to $N_g^b\sim 4$. Such a trend

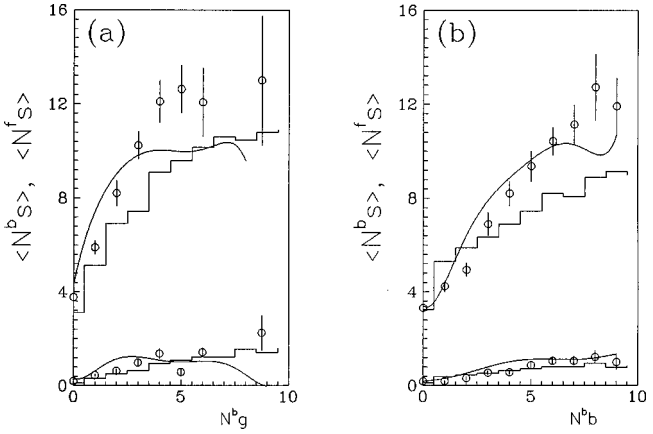

FIG. 4. (a) The correlations between forward-backward s particles (N_s^f,N_s^b) and the backward g particles (N_g^b). (b) The dependence of $\langle N_s^f\rangle$ and $\langle N_s^b\rangle$ on backward b particles (N_b^b) for the reaction under study. The error bars denote the experimental data. The histograms and the solid curves denote ICM and modified FRITIOF calculations, respectively.

could be understood by processes in the spectator parts. Starting from $N_g^b>4$, the interactions on the heavy emulsion nuclei are weakly connected to the process of hadronic production.

For $N_g^b<4$, the modified FRITIOF predictions compared with ICM calculations are in better accord with the experimental N_s^f (N_g^b) correlation. This may imply that the hardening of the calculated meson spectrum in the ICM (in the region $N_g^b<4$) can be achieved when the production and interactions of resonances are taken into account. For $N_g^b>4$, the modified FRITIOF model and ICM theoretical calculations agree between themselves and both underpredict the experimental data. In the region $N_g^b>4$, the main contribution to the s-particles multiplicity is interactions with heavy emulsion nuclei. Additional hadron production in this region could be achieved by creating extra strings between quarks of the colliding hadrons.

In the BHS, the ICM calculations provide a better description for the experimental $\langle N_s^b\rangle$ as a function of N_g^b.

In the same figure the correlations between the average number of s particles in both hemispheres ($\langle N_s^f\rangle$ and $\langle N_s^b\rangle$) and the multiplicity of backward b particles (N_b^b) are presented. In both models, the s particles are related to the excitation energy of the nucleus (through the dependence of the participant nucleons of the two colliding nuclei on cascade particles) and thus in an indirect way to the evaporated b particles. Both models describe rather well the $\langle N_s^b\rangle$ dependence on N_b^b. In contrast to the measured correlations, where the $\langle N_s^f\rangle$ dependence on N_b^b is nearly linear, the ICM calculations show that such a variation is rather weak. The modified FRITIOF model fairly reproduces the $\langle N_s^f\rangle$ dependence on N_b^b. Thus, an incorrect calculation of the excitation energy in the ICM accounts for the obtained discrepancy of the $N_s^f(N_b^b)$ correlation.

As stated earlier, the g particles multiplicity is directly proportional to the total number of participant nucleons in the two nuclei. In addition, the g-particles contribute to the excitation of the residual nucleus and are therefore, related

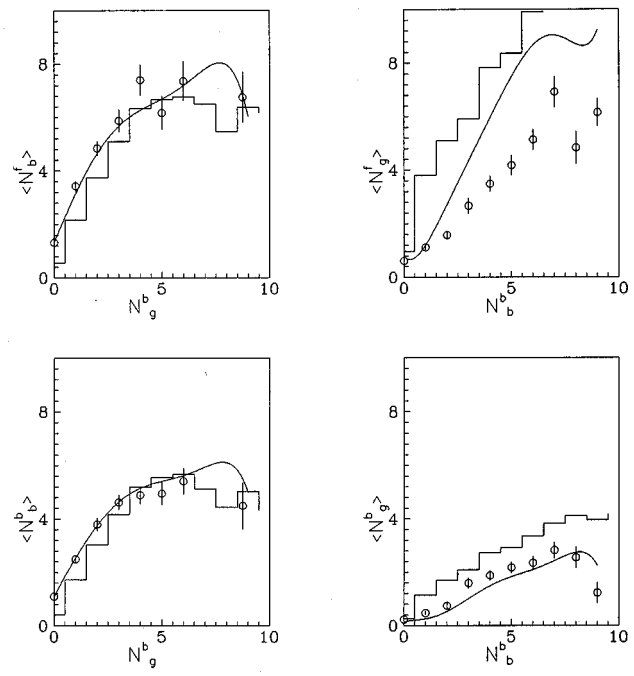

FIG. 5. On the left hand side, the correlations between forward-backward b particles (N_b^f, N_b^b) and the backward g particles (N_g^b). On the right hand side, the dependence of ($\langle N_g^f \rangle, \langle N_g^b \rangle$) on backward b particles (N_b^b) for the reaction under study. The notation is the same as in Fig. 4.

indirectly to the multiplicity of evaporated b particles. Thus a study of slow particle production as a function of N_g^b will reveal the impact parameter dependence.

Figure 5 exhibits the dependence of both the average number of b particles in the forward ($\langle N_b^f \rangle$) and backward ($\langle N_b^b \rangle$) hemispheres on the number of backward g particles (N_g^b). By inspection of the figure one notices the following.

(i) The experimental and calculated values of $\langle N_b^{f(b)} \rangle$ increase with increasing $N_g^b \sim 4$, which turns into a saturation for large N_g^b values. The saturation seen in $\langle N_b^{f(b)} \rangle$ at medium and small impacts is a consequence of the finite size of the projectile nucleus.

(ii) The ICM adequately describes the saturation seen in $N_b^{f(b)}$ (N_g^b) correlation.

(iii) For $N_g^b < 4$, the ICM calculations show smaller average b particles than experimentally observed. Events with $N_g^b < 4$ are dominated by interactions with light nuclei.

(iv) The modified FRITIOF calculations markedly reproduce the $\langle N_b^b \rangle$ and the $\langle N_b^f \rangle$ dependence on N_g^b.

In the same figure we examine how $\langle N_g^f \rangle$ and $\langle N_g^b \rangle$ depend on N_b^b. An increase in the number of backward b particles, N_b^b, is accompanied by a fast increase in the multiplicity of forward g particles ($\langle N_g^f \rangle$) for the reaction under study. The modified FRITIOF calculations are in better accord with the experimental data in the case of the $\langle N_g^b \rangle$ dependence on N_b^b. However, in the case of $\langle N_g^f \rangle$ as a function of N_b^b, both calculations reflect such a dependence in a manner stronger than do the experimental data.

Finally in Fig. 6 the connection between the forward-backward g- and b-particle production is illustrated. In the case of N_b^f (N_b^b) correlation, the ICM deviates from the experimental data at the very small and large N_b^b values. The modified FRITIOF model fairly describes such correlation. As for N_g^f (N_g^b) correlation, both calculations deviate from the experimental results.

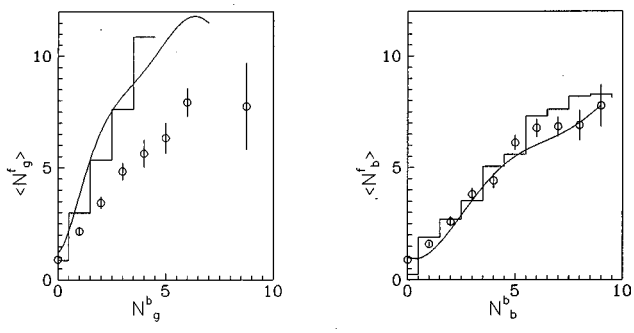

FIG. 6. On the left hand side, the correlations between forward (N_g^f) and backward (N_g^b) g particles for the reaction under study. On the right hand side, the dependence of forward b particles (N_b^f) on the backward b particles ($\langle N_b^b \rangle$). The notation is identical to Fig. 4.

From Figs. 5 and 6 we conclude that both models assume more strong forward collimation of g particles than experiment. The yield of g particles in the forward region can be reduced by taking into account the effect of the coalescence of nucleons (i.e., the formation of the light nuclear fragments, d, t, ^{3}He, and ^{4}He from nucleons that are close in phase space), which is disregarded in the two models used here. As one can see from the N_g^f (N_b^b) and N_g^f (N_g^b) correlations, the importance of this effect increases with increasing the multiplicity of particles in the forward cone.

IV. CONCLUSION

In this work, a comparison of experimental results on yields of s, g, and b particles (fast and slow hadrons) in the forward and backward hemispheres, resulting from the interactions of ^{6}Li with emulsion nuclei at 3.7A GeV, is made with two theoretical models: a typical intranuclear cascade model and modified FRITIOF model. The latter model consists of two main ingredients: (i) the distribution of the nucleons knocked out by hard collisions based on a classical Glauber approach and (ii) the description of the secondary interactions by soft processes (Reggeon interactions) which amounts to a cascade on the plane of impact parameter. Particles taking part in the hard processes become excited strings as in the FRITIOF model. From such comparison the following conclusions can be drawn.

(i) The ICM describes the emission of backward s particles, but underpredicts the forward s-particle emission.

(ii) The ICM shows an excess of knocked-out protons (g particles) in the two hemispheres.

(iii) The ICM underpredicts the emission of b particles in both hemispheres for light nuclei.

(iv) The ICM can describe the correlations between particles emitted in the BHS [except for the N_g^b (N_b^b) correlation]. On the other hand, for the correlations between backward and forward particles, the model can only predict the b-particle correlation.

(v) The modified FRITIOF model reproduces the multiplici-

ties and correlations of the emitted particles in the two hemispheres.

(vi) Neither of the used models can reproduce the N_g^f (N_b^b) and N_g^f (N_g^b) dependences.

Thus, even though the present data lie in the range of applicability of the ICM, there are problems concerning a correct description of particle cascading and the evaluation of excitation energy given to the residual nucleus. The overall good agreement between the modified FRITIOF model and the experimental data suggests that the Reggeon picture can be considered as a plausible alternative to modern approaches [3,22] in describing nuclear cascading.

ACKNOWLEDGMENTS

The author acknowledges Professor V.V. Uzhinskii for his guidance and continuous help.

[1] EMU01 Collaboration, M. I. Adamovich *et al.*, Z. Phys. A **358**, 337 (1997).
[2] EMU01 Collaboration, M. I. Adamovich *et al.*, Phys. Lett. B **407**, 92 (1997).
[3] A. Ferrari, J. Ranft, S. Roesler, and P. R. Sala, Z. Phys. C **71**, 75 (1996).
[4] EMU01 Collaboration, M. I. Adamovich*et al.*, Z. Phys. C **65**, 421 (1995).
[5] EMU01 Collaboration, M. I. Adamovich *et al.*, Phys. Lett. B **363**, 230 (1995).
[6] EMU01 Collaboration, M. I. Adamovich *et al.*, Nucl. Phys. **A593**, 535 (1995).
[7] M. El-Nadi, A. Abdelsalam, N. Ali-Mossa, Z. abou-Moussa, S. Kamel, Kh. Abdel-Waged, W. Osman, and B. Badawy, Eur. Phys. J. A **3**, 183 (1998).
[8] M. El-Nadi, A. Abdelsalam, N. Ali-Mossa, Z. abou-Moussa, Kh. Abdel-Waged, W. Osman, and B. Badawy, Nuovo Cimento A (to be published).
[9] S. Yu. Shmakov, V. V. Uzhinskii, and A. M. Zadorozhny, Comput. Phys. Commun. **54**, 125 (1989).
[10] Kh. Abdel-Waged and V. V. Uzhinskii, Phys. At. Nucl. **60**, 828 (1997).
[11] Kh. Abdel-Waged and V. V. Uzhinskii, J. Phys. G **24**, 1723 (1998).
[12] M. El-Nadi, A. Abdel-Salam, A. Hussein, E. A. Shaat, N. Ali-Mousa, Z. Abou-Mousa, S. Kamel, Kh. Abdel-Waged, and E. El-Falaky, Int. J. Mod. Phys. E **6**, 191 (1997).
[13] B. Nilsson-Almqvist and E. Stenlund, Comput. Phys. Commun. **43**, 387 (1987).
[14] V. Weisskopf, Phys. Rev. **52**, 295 (1937); W. A. Friedman, Phys. Rev. C **28**, 16 (1983).
[15] V. S. Barachenkov, F. G. Zhergi, and Zh. Zh. Muslamanbekov, JINR Report No. R2-83-117, Dubna, 1983; V. D. Toneev and K. K. Gudima, Nucl. Phys. **A400**, 173 (1983); **A401**, 329 (1983).
[16] V. V. Uzhinskii and A. S. Pak, Phys. At. Nucl. **59**, 1064 (1996).
[17] V. S. Barachenkov, K. K. Gudima, and V. D. Toneev, Acta Phys. Pol. **36**, 260 (1969).
[18] V. S. Barachenkov *et al.*, Nucl. Phys. **A187**, 531 (1972).
[19] S. G. Mashnik, in Proceedings of a Specialist's Meetings on Intermediate Energy Nuclear Data: Models and Codes, Paris, 1994, p. 107.
[20] B. M. Blann, H. Gruppelaar, P. Nagel, and J. Rodens, ''Intermediate code comparison for intermediate energy nuclear data,'' NEA, OECD, report, Paris, 1994.
[21] K. G. Boreskov, A. B. Kaidalov, S. T. Kiselev, and N. Ya. Smorodinskaya, Yad. Fiz. **53**, 569 (1991) [Sov. J. Nucl. Phys. **53**, 356 (1991)].
[22] K. Werner, Phys. Rep. **232**, 87 (1993).
[23] S. Yu. Shmakov, N. V. Slavin, and V. V. Uzhinskii, JINR Report No. E2-88-792, Dubna, 1988.
[24] D. Armutlisky *et al.*, Z. Phys. A **328**, 455 (1987).
[25] H. N. Agakishiev *et al.*, Yad. Fiz. **56**, 170 (1993) [Sov. J. Nucl. Phys. **56**, 1397 (1993)].
[26] A. A. Baldin, Yad. Fiz. **56**, 174 (1993) [Sov. J. Nucl. Phys. **56**, 385 (1993)].
[27] A. Schuettauf *et al.*, Nucl. Phys. **A607**, 457 (1996).
[28] I. Dostrovsky, Z. Frankel, and G. Friedlandel, Phys. Rev. **116**, 683 (1959).